



Research Article

THERMO-ELASTOPLASTIC SOLUTIONS OF A THICK-WALLED TUBE WITH FIXED ENDS SUBJECTED TO A TEMPERATURE CYCLE FROM ITS INNER SURFACE

Yasemin KAYA*¹, Ahmet N. ERASLAN²

¹Middle East Technical University, Dep. of Engineering Sciences, ANKARA; ORCID:0000-0002-3067-1783

²Middle East Technical University, Dep. of Engineering Sciences, ANKARA; ORCID:0000-0002-1158-0042

Received: 30.01.2018 Revised: 23.07.2018 Accepted: 30.08.2018

ABSTRACT

A thermo-elastoplastic response of a long tube under periodic temperature cycle from its inner surface is analyzed. The temperature of the inner surface increases linearly with time, remains constant for a while at a maximum value, and then cools down linearly to the initial temperature. Thermo- elastic and plastic stress distributions in the tube under these conditions are determined through analytical means. Plastic stress states are treated using Tresca's yield criterion. The tube undergoes elastic, elastoplastic and unloading stages during the temperature cycle.

Keywords: Thick-walled tube, transient heat conduction, temperature cycle, thermal stress, thermoelastoplasticity, sudden unloading.

1. INTRODUCTION

Cylindrical elements are widely used in many high temperature applications such as in heat generators, aerospace applications, boilers and nuclear reactors. For this reason, elastic and elastoplastic analyses of these structures are an important engineering issue to design more reliable structures. This issue has attracted the attention of many experts and researchers.

Elastic stresses occurring due to time-dependent temperature distribution in tubes under different boundary conditions have been obtained by analytical and numerical methods. Segall [1] derived the closed-form solution for the axisymmetric thick-walled tube under an arbitrary internal thermal loading which is in the form of a polynomial, and with convection on the surrounding external environment. Radu et al. [2] developed a set of analytical solutions for temperature field and the associated elastic thermal stress distributions in a hollow cylinder with traction free surfaces. A sinusoidal thermal load is applied to the inner surface of the cylinder and the solution of temperature distribution is achieved by applying Henkel transform to the integral form. Shahani and Nabavani [3] solved the quasi-static thermoelasticity problem of a thick-walled cylinder using the finite Henkel transform for the differential equations of both temperature and displacements. Kim and Noda [4] analyzed a thermoelastic problem which included a two-dimensional unsteady temperature field and associated thermal stress in an infinite hollow

* Corresponding Author: e-mail: yaseminkayatr@gmail.com, tel: (312) 210 23 82

cylinder. They used the Green's function approach based on the laminate theory to obtain the temperature field and thermoelastic potential function, and Mitchell's function to obtain thermoelastic stresses. Kaya and Eraslan [5] derived an analytical solution to analyze the thermoelastic behavior of long tube with free ends under a periodic heat loading from its inner surface. The analytical results were compared to those of a numerical solution based on a combination of collocation and shooting methods. They also calculated the axial strain for different values of the wall thickness. The axial strain is larger in the thin tubes.

Plastic deformation makes the solution of the problem more complicated. Orcan and Eraslan [6] performed a numerical solution to the thermo-elastoplastic deformation of internal heat-generating tubes by considering the thermomechanical coupling effect and the temperature-dependent physical properties of the material. It has been seen that the thermomechanical coupling effect is negligible for this specific problem. However, it should be included at early times of the unsteady behavior of systems due to the rapid increase in temperatures. Additionally, it has been shown that the temperature dependence of the mechanical and thermal properties of the material influences the computed profiles significantly; therefore, it should be considered in similar models [7]. Jahanian and Sabbaghian [8] and Jahanian [9] presented the thermo-elastoplastic analysis of a long hollow cylinder with temperature dependent material properties. The tube is subjected to rapid heating and cooling for linear and nonlinear hardening cases. Plastic deformation was treated numerically.

Arslan et al. [10] analytically examined the elastoplastic behavior of a long solid cylinder which was subjected to a temperature cycle from its outer surface. The temperature cycle shows an increasing, constant and decreasing trend as a linear function of time. Eraslan and Apatay [11] developed an analytical model to predict elastic, partially plastic, and plastically predeformed elastic states of stress in a long cylinder which was subjected to periodic surface heating. Based on the Tresca's yield criterion, associated flow rule, the generalized plane strain and linearly hardening material behavior, they formulated two different elastic and two different plastic regions.

Analytical solution of the thick-walled tube is complicated compared to solid cylinder problem due to its geometry and containing various integrals of Bessel functions. In this paper, the thermo-elastoplastic response of a long tube with fixed ends has been analytically examined. The tube is initially at zero temperature. For times $t > 0$, the inner surface of the tube is subjected to a cycle, while the outer surface is isolated. An uncoupled solution has been carried out since the tube is heated and cooled down slowly. The plastic zone has been modeled using the Tresca criterion based on the plane strain assumption and perfectly plastic material property. Numerical results for stresses, strains, and displacement distributions have been presented for one temperature cycle.

2. TEMPERATURE DISTRIBUTION

A long tube of inner radius a and outer radius b is considered in cylindrical polar coordinate system. Cylindrical symmetry is assumed. As the tube is long and symmetric in θ -direction, the transient heat conduction equation becomes one-dimensional and reads [12]

$$\frac{\partial^2 T}{\partial r^2} + \frac{1}{r} \frac{\partial T}{\partial r} = \frac{1}{\kappa} \frac{\partial T}{\partial t}; \quad a < r < b, \quad t > 0, \quad (1)$$

where T is temperature, r radial coordinate, $\kappa (= k / \rho C)$ thermal diffusivity, and t time. Initial and boundary conditions take the forms

$$T(r, 0) = 0, \quad a \leq r \leq b, \quad (2)$$

$$T(a, t) = f(t), \quad k \frac{\partial T}{\partial r}(b, t) = 0, \quad t > 0, \quad (3)$$

where k is the coefficient of thermal conductivity, $f(t)$ represents the function of temperature cycle shown in Fig. 1 and described with time as

$$f(t) = \begin{cases} (T_m / t_t)t & \text{for } 0 < t \leq t_t \\ T_m & \text{for } t_t < t \leq t_t + t_c \\ T_m - (T_m / t_t)(t - t_t - t_c) & \text{for } t_t + t_c < t \leq 2t_t + t_c \\ 0 & \text{for } t > 2t_t + t_c \end{cases} \quad (4)$$

where T_m represents the maximum temperature.

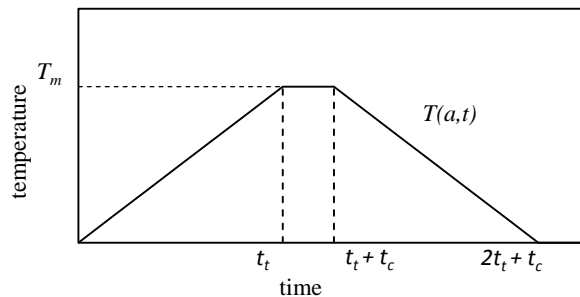


Figure 1. Temperature cycle applied to the inner surface of the tube.

Assuming the tube is initially at zero temperature, the heat conduction equation is solved by the application of Duhamel's theorem [12, 13] and temperature field in the radial direction in the tube is obtained as

$$T(r,t) = \frac{T_m}{t_t}t + \frac{T_m\pi}{t_t\kappa} \sum_{n=1}^{\infty} \left(1 - e^{-\kappa\lambda_n^2 t}\right) \frac{C_0(r,\lambda_n)}{\lambda_n^2 F(\lambda_n)} P(\lambda_n), \quad (5)$$

where

$$\begin{aligned} C_0(r,\lambda_n) &= J_0(r\lambda_n)Y_0(a\lambda_n) - Y_0(r\lambda_n)J_0(a\lambda_n), \\ F(\lambda_n) &= J_0(a\lambda_n)^2 - J_1(b\lambda_n)^2, \\ P(\lambda_n) &= J_1(b\lambda_n)^2, \end{aligned} \quad (6)$$

and J and Y are Bessel functions of a first and second kind, respectively, and λ_n is the positive roots of the following eigenvalue equation

$$\lambda [J_0(a\lambda)Y_1(b\lambda) - Y_0(a\lambda)J_1(b\lambda)] = 0. \quad (7)$$

3. ELASTIC SOLUTION

The tube has stress free inner surface and radially constrained outer surface. In the analysis, elastic region obeys Hook's law. Equation of equilibrium reads [14]

$$d\sigma_r / dr + (\sigma_r - \sigma_\theta) / r = 0, \quad (8)$$

Using strain-displacement relations ($\varepsilon_r = du / dr$ and $\varepsilon_\theta = u / r$), the constitutive equations are written in terms of radial and circumferential stresses and displacement. Substituting these stresses into Eq. (8), the governing equation for the displacement can be derived as the following:

$$u = C_1 r + \frac{C_2}{r} + \frac{(1+\nu)\alpha}{(1-\nu)r} \int rT(r,t)dr, \tag{9}$$

where u is the radial displacement, C_1 and C_2 are arbitrary integration constants, α coefficient of thermal expansion, and ν represents the Poisson's ratio. Substituting the radial displacement found above into the stress-displacement equations, radial and circumferential stresses are derived as

$$\sigma_r = \frac{2G}{1-2\nu} C_1 - \frac{2GC_2}{r^2} - \frac{2G\alpha(1+\nu)}{(1-\nu)r^2} \int rT(r,t)dr, \tag{10}$$

$$\sigma_\theta = \frac{2G}{1-2\nu} C_1 + \frac{2GC_2}{r^2} + \frac{2G\alpha(1+\nu)}{(1-\nu)} \left(\frac{1}{r^2} \int rT(r,t)dr - T(r,t) \right). \tag{11}$$

Mechanical boundary conditions for internally free and radially constraint tube are: at $r = a$, $\sigma_r = 0$ and at $r = b$, $u = 0$. Solving the Eqs. (10) and (11), for C_1 and C_2 with the use of the boundary conditions, one can obtain the integration constants as

$$C_1 = -\frac{\alpha(1-\nu-2\nu^2)}{(1-\nu)[a^2+b^2(1-2\nu)]} \int_a^b rT(r,t)dr, \tag{12}$$

$$C_2 = -\frac{a^2\alpha(1+\nu)}{(1-\nu)[a^2+b^2(1-2\nu)]} \int_a^b rT(r,t)dr, \tag{13}$$

4. ELASTOPLASTIC SOLUTION

As seen in Fig. (3), the stress state is: $\sigma_r > \sigma_z > \sigma_\theta$. Hence, Tresca's yield criterion is $\sigma_r - \sigma_\theta = \sigma_y$, and the associated flow rule takes the form $\varepsilon_\theta^p = -\varepsilon_r^p$ and $\varepsilon_z^p = 0$. Here, σ_y represents the yield stress which is considered as a function of temperature given by the equation $\sigma_y = \sigma_{th} = \sigma_0(1 - \beta T)$,

where β is a constant. Substituting the stresses into Eq.(14) and using the flow rule, ε_r^p can be also written in terms of the radial displacement. Thus, radial and circumferential stresses are derived in terms of the displacement as the following

$$\sigma_r = \frac{1}{2(1-2\nu)} [2Gu + 2Gru' + r(1-2\nu)\sigma_0 - (4Gr\alpha(1+\nu) + r\beta\alpha(1-2\nu)\sigma_0)T(r,t)], \tag{15}$$

$$\sigma_\theta = \frac{1}{2r(1-2\nu)} [2Gu + 2Gru' - r(1-2\nu)\sigma_0 - (4Gr\alpha(1+\nu) - r\beta\alpha(1-2\nu)\sigma_0)T(r,t)]. \tag{16}$$

Substituting the stresses into the equation of equilibrium, the nonhomogeneous Euler equation is obtained for the radial displacement:

$$r^2 \frac{d^2u}{dr^2} + r \frac{du}{dr} - u = \frac{r}{2G} [2(1-2\nu)\sigma_0(\beta T(r,t) - 1) + (4G\alpha(1+\nu) + \beta(1-2\nu)\sigma_0)rT'(r,t)]. \quad (17)$$

The homogeneous solution can be readily obtained while the particular solution is obtained by the variation of the parameters. General solution for the radial displacement in the plastic zone is obtained in the form of

$$u = C_3 r + \frac{C_4}{r} + \frac{r(1-2\nu)\sigma_0}{2G} \left(\beta \int_a^r \frac{T(\xi)}{\xi} d\xi + \frac{1-2\ln(r)}{2} \right) + \frac{2\alpha(1+\nu)}{r} \int_a^r \xi T(\xi) d\xi. \quad (18)$$

Substituting the radial displacement into the stress-displacement equations, Eqs. (15) and (16), radial and circumferential stresses in the plastic zone are obtained as

$$\sigma_r = \frac{2GC_3}{1-2\nu} + \beta\sigma_0 \int_a^r \frac{T(\xi,t)}{\xi} d\xi + \frac{\sigma_0}{2}(1-2\ln(r)), \quad (19)$$

$$\sigma_\theta = \frac{2GC_3}{1-2\nu} + \beta\sigma_0 \left[\int_a^r \frac{T(\xi,t)}{\xi} d\xi + T(r,t) \right] - \frac{\sigma_0}{2}(1+2\ln(r)), \quad (20)$$

and, radial plastic strain can be derived as

$$\varepsilon_r^p = -\frac{C_4}{r^2} - \frac{2\alpha(1+\nu)}{r^2} \int_a^r \xi T(\xi,t) d\xi + \left(\alpha(1+\nu) + \frac{(1-\nu)\beta}{2G} \right) T(r,t) - \frac{(1-\nu)\beta}{2G} \sigma_0. \quad (21)$$

Since $\varepsilon_z^p = 0$, axial stress can be expressed in terms of radial and circumferential stresses. Elastic equations derived in the first part can be used in the elastoplastic analysis. Representing the elastic-plastic border by r_1 , boundary and interface conditions are written as: $\sigma_r^p(a) = 0, u_r^e(b) = 0; \sigma_r^p(r_1) = \sigma_r^e(r_1), u_r^p(r_1) = u_r^e(r_1)$. Here, p and e denote plastic and elastic regions. By using these conditions, integration constants, $C_i (i = 1, 4)$, are represented by r_1 . It can be calculated the location of the elastic-plastic border using the condition of at $r = r_1, \varepsilon_r^p = 0$.

5. SOLUTION OF UNLOADED REGION

At a time $t = t_u$, the increase of the plastic strains ceases at $r = a$. After that time, unloading starts and the unloaded region moves very quickly to the outer of the tube. At a time $t = t_u$, unloading criterion for a constant radial coordinate r is $(\partial\varepsilon(r,t)/\partial t)|_{r=t_u} = 0$. Since the unloaded region propagates very quickly, a sudden unloading assumption is adopted in the formulation. Therefore, for times $t > t_u$, plastic strains at a radial coordinate in $a < r \leq r_u$ are assumed to be constant and equal to the values calculated at time $t = t_u$.

The tube is elastic in $r_u < r < b$ and the elastic equations are valid in this region. Field equations for the unloaded region are calculated as the following:

$$u = C_5 r + \frac{C_6}{r} + \frac{1}{1-\nu} \left[(1+\nu) \frac{\alpha}{r} \int_a^r \xi T(\xi,t) d\xi + (1-2\nu)r \int_a^r \frac{\varepsilon_r^p}{\xi} d\xi \right], \quad (22)$$

$$\sigma_r = \frac{2G}{1-2\nu} C_5 - \frac{2GC_6}{r^2} + \frac{2G}{1-\nu} \int_a^r \frac{\varepsilon_r^p}{\xi} d\xi - \frac{2G\alpha(1+\nu)}{(1-\nu)r^2} \int_a^r \xi T(\xi,t) d\xi, \quad (23)$$

$$\sigma_{\theta} = \frac{2G}{1-2\nu} C_5 + \frac{2GC_6}{r^2} + \frac{2G}{1-\nu} \left(\int_a^r \frac{\varepsilon_r^p}{\xi} d\xi + \varepsilon_r^p \right) + \frac{2G\alpha(1+\nu)}{(1-\nu)} \left(\frac{1}{r^2} \int_a^r \xi T(\xi, t) d\xi - T(r, t) \right), \quad (24)$$

where C_5 and C_6 are the integration constants to be calculated using the interface conditions: at $r = r_u$, $u = u_e$ and $\sigma = \sigma_e$.

6. NUMERICAL RESULTS

Numerical results are given for the following nondimensional and normalized variables: Time: $\tau = \alpha t / b^2$, material parameter: $\bar{\beta} = \beta / T_m$, temperature: $\bar{T} = T / T_m$, inner radius: $\bar{a} = a / b$, normal stress: $\bar{\sigma} = \sigma / \sigma_0$, normal strain $\bar{\varepsilon} = \varepsilon G / \sigma_0$, radial displacement: $u = uG / \sigma_0 b$, heat load parameter $q = \alpha T_m G / \sigma_0$. Numerical results are given for the parameters $\tau_i = 1.2$, $\tau_e = 0.3$, $\bar{a} = 0.2$, $\nu = 0.3$, $\beta = 0.2$, and $q = 0.2$. Fig. (2) shows the nondimensional temperature distribution in the radial direction in the tube.

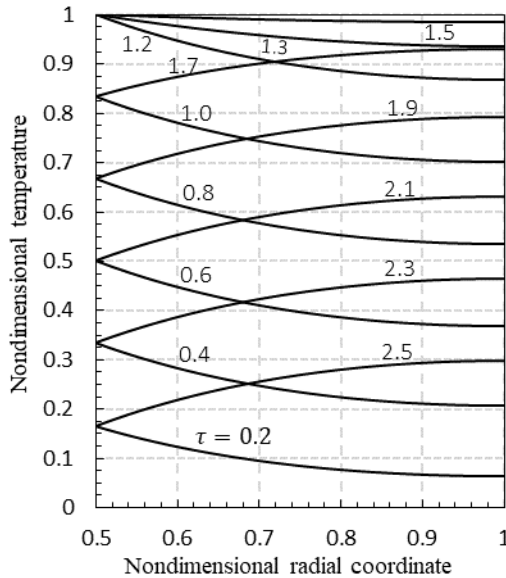


Figure 2. Temperature distribution in the tube during one temperature cycle.

The tube is fully elastic between $\tau = 0 - 0.725$. Elastic stresses and displacement are given in Fig. (3). The magnitudes of the stress distributions in the elastic region are close to each other.

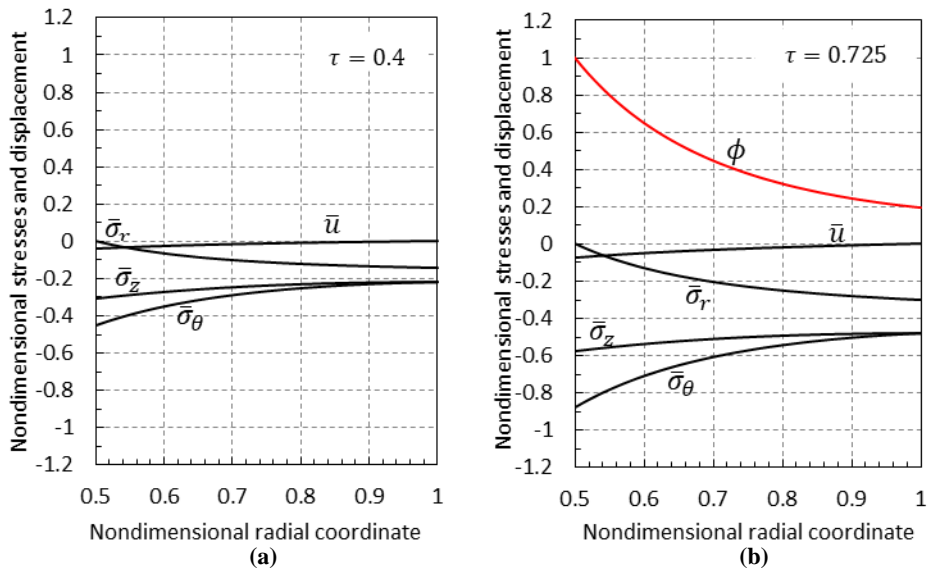


Figure 3. Stress and displacement distributions at the elastic stage at (a) $\tau = 0.4$, and (b) $\tau = 0.725$.

With the increasing temperature, the magnitude of the axial and circumferential stress components increase with respect to the radial stress component and the difference between them gets larger. At time $\tau = 0.725$, the maximum difference between the radial and circumferential stresses equals to the temperature dependent yield stress at the inner surface of the tube. At this point, the tube undergoes plastic deformation at its inner surface. Tresca's yield criterion is used to determine the onset of the plastic deformation. The plastic region, then, progresses outwards in time. The stresses, strains and displacement distribution in the tube at the elastoplastic stage are shown in the Fig. (4).

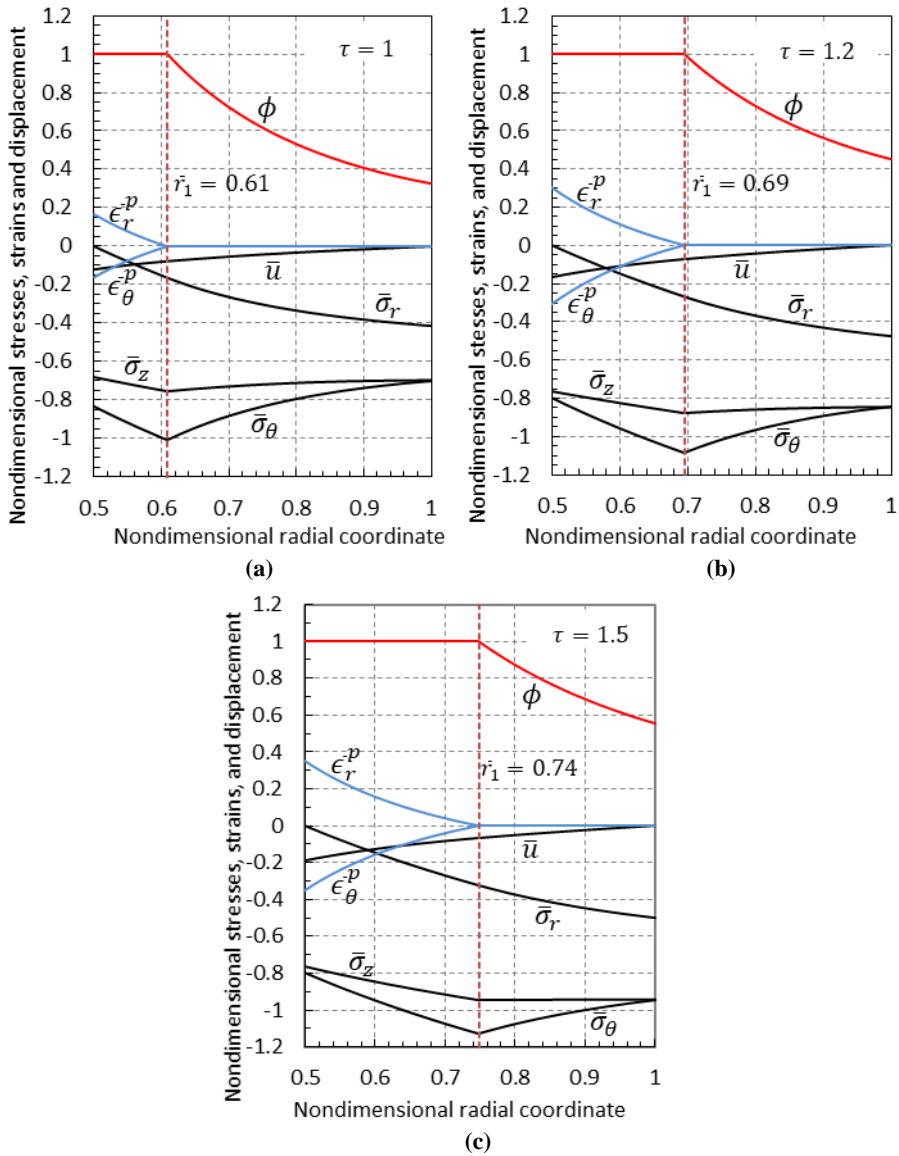


Figure 4. Stresses, plastic strains and displacement distributions of the elastoplastic stage at (a) $\tau = 1.0$, (b) $\tau = 1.2$, and (c) $\tau = 1.5$.

In this figure, $\phi = \sigma_y / \sigma_{th}$, and when $\phi < 1$, the tube is elastic. When $\phi \geq 1$, it undergoes plastic deformation. The integral of $\int_a^r \frac{T(\xi, t)}{\xi} d\xi$ which appears in the equations of the plastic stage is evaluated using the Simpson's method. At $\tau = 1.5$, the increase in plastic strain ceases at $r = a$. After that time, an unloaded region emerges from the inner surface. As the unloaded region

spreads out to the outwards very fast, a sudden unloading assumption is made to model the behavior of tube after time $\tau=1.5$. According to the sudden unloading assumption, the elastic-plastic border after the times $\tau=1.5$ is accepted as the unloaded-elastic border. Therefore, after that time, the plastic strains at each radial coordinate in the unloaded region are constant, in other words, frozen; and they equal to the plastic strains in the plastic region at time $\tau=1.5$. Stresses and displacement distributions for the unloaded stage of the tube are shown in Fig. (5).

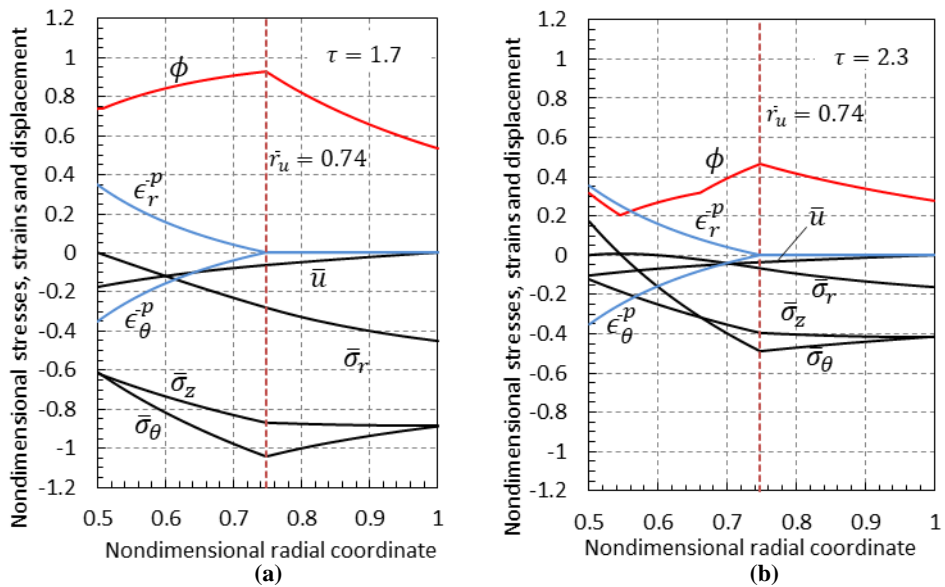


Figure 5. Stresses, plastic strains and displacement distributions of the unloaded stage at (a) $\tau = 1.7$, and (b) $\tau = 2.3$.

7. CONCLUDING REMARKS

An uncoupled thermo-elastoplastic analysis of a long tube with fixed ends has analytically been carried out based on (i) plane strain condition, (ii) perfectly plastic material property, (iii) Tresca's yield criterion and associated flow rule, and (iv) temperature dependent yield strength. The tube is externally isolated and subjected to a temperature cycle from its inner surface. Using Duhamel's theorem, the temperature distribution in the radial direction in the tube is obtained for one temperature cycle. Then, stress, strain and displacement distributions in the tube are calculated. The tube undergoes elastic, elastoplastic and unloading stages during the temperature cycle. All the calculated stresses show compressive behavior in the tube.

REFERENCES

- [1] A. E. Segall, (2004) Thermoelastic stresses in an axisymmetric thick-walled tube under an arbitrary internal transient, *J. of Press. Ves. Tech.* 126, 327-332.
- [2] V. Radu, N. Taylor, E. Paffumi, (2008) Development of new analytical solutions for elastic thermal stress components in a hollow cylinder under sinusoidal transient thermal loading, *Int. J. of Press. Ves. and Pip.* 85, 885-893.

- [3] A. R. Shahani, S. M. Nabavi, (2007) Analytical solution of the quasi-static thermoelasticity problem in a pressurized thick-walled cylinder subjected to transient thermal loading, *Applied Mathematical Modeling* 31, 1807-1818.
- [4] K. S. Kim, N. Noda, (2002) Green's function approach to unsteady thermal stresses in an infinite hollow cylinder of functionally graded material, *Acta Mechanica* 156:3-4, 145-161.
- [5] Y. Kaya, A.N. Eraslan, (2004) Thermoelastic response of a long tube subjected to periodic heating, *Mathematical Sciences and Applications E-Notes (MSAEN)* 2, 14-27.
- [6] Y. Orcan, A. N. Eraslan, (2001) Thermal Stresses in Elastic-Plastic Tubes with Temperature-Dependent Mechanical and Thermal Properties, *Journal of Thermal Stresses* 24:11, 1097-1113.
- [7] A.N. Eraslan, Y. Orçan, (2002) Computation of transient thermal stresses in elastic-plastic tubes: Effect of coupling and temperature-dependent physical properties, *J. of Thermal Stresses* 25, 559-572.
- [8] S. Jahanian, M. Sabbaghian, (1990) Thermoelastoplastic and residual stresses in a hollow cylinder with temperature-dependent properties, *J. of Pres. Ves. Tech.* 112, 85-91.
- [9] S. Jahanian, (1996) Thermoelastoplastic stress analysis of a thick-walled tube of nonlinear strain hardening, *Transactions of the ASME* 118, 340-346.
- [10] E. Arslan, W. Mack, A. N. Eraslan, (2008) Effect of a temperature cycle on a rotating elastic-plastic shaft, *Acta Mechanica* 195, 129.
- [11] A.N. Eraslan, T. Apatay, (2016) Analytical solution to thermal loading and unloading of a cylinder subjected to periodic surface heating, *J. Thermal Stresses* 39:8, 928-941.
- [12] D.W. Hahn, M.N. Özışık, (2012) Heat Conduction, *John Wiley and Sons*, Hoboken, NJ.
- [13] H. S. Carslaw, J. C. Jaeger, (1959) Conduction of Heat in Solids, *Oxford University Press*, Oxford.
- [14] W. Johnson, P. B. Mellor, (1970) Plasticity for Mechanical Engineers, *D. van Nostrand Company*, Great Britain.